Microstructured gradient-index lenses for THz photoconductive antennas

Brincker, Mads; Karlsen, Peter ; Skovsen, Esben; Søndergaard, Thomas

Published in:
AIP Advances

DOI (link to publication from Publisher):
10.1063/1.4942426

Publication date:
2016

Document Version
Publisher's PDF, also known as Version of record

AIP Advances

Microstructured gradient-index lenses for THz photoconductive antennas

Mads Brincker, Peter Karlsen, Esben Skovsen, and Thomas Søndergaard

Citation: AIP Advances **6**, 025015 (2016); doi: 10.1063/1.4942426
View online: http://dx.doi.org/10.1063/1.4942426
View Table of Contents: http://scitation.aip.org/content/aip/journal/adva/6/2?ver=pdfcov
Published by the AIP Publishing

Microstructured gradient-index lenses for THz photoconductive antennas

Mads Brincker,[1] Peter Karlsen,[2] Esben Skovsen,[1]
and Thomas Søndergaard[1,a]
[1]*Department of Physics and Nanotechnology, Aalborg University, Skjernvej 4A, DK-9220 Aalborg East, Denmark*
[2]*School of Physics and Astronomy, University of Exeter, Stocker Road, Exeter EX4 4QL, UK*

(Received 2 October 2015; accepted 5 February 2016; published online 16 February 2016)

A new type of substrate lens for photoconductive antennas (PCA's) based on sub-wavelength microstructuring is presented and studied theoretically by the use of Greens function integral equation methods (GFIEM's). By etching sub-wavelength trenches into a flat substrate, the effective dielectric constant can be designed to function like a gradient index (GRIN) lens. The proposed GRIN substrate lenses have sub-mm dimension, which is smaller than the dimensions of a typical hyper-hemispherical substrate lens (HSL), and could enable fabrication of arrays of closely packed PCA's with individual lenses integrated directly into the PCA substrate. The performance of different GRIN lenses is compared to a HSL and shown to be comparable with regards to the terahertz radiation extraction efficiency, and it is shown that the collimating properties of these GRIN lenses can be tailored by changing the parameters used for microstructuring.
[http://dx.doi.org/10.1063/1.4942426]

I. INTRODUCTION

Imaging and spectroscopy in the THz range of the electro-magnetic spectrum has, since the demonstration of the first THz time-domain spectrometer (THz-TDS),[1] become an increasingly popular method to study a wide range of biological, chemical and physical systems.[2] THz-TDS systems and continuous-wave terahertz frequency-domain spectrometers often use PCA's as both source and detector of THz radiation. However, due to the inherent design of a typical PCA, a large part of the emitted THz radiation is trapped within the semiconductor substrate. To avoid this, it is customary to mount a HSL to the PCA to out-couple and collimate the radiation,[3,4] as illustrated in Fig. 1(a). However, the large size of typical HSL's limits the integrability by adding considerable bulk to the PCA and prevents close packing of many individual PCA's into PCA micro-arrays. In addition HSL's are sensitive to mis-alignment.[5] PCA arrays have shown to produce record breaking power levels,[6] allow for beam steering,[7] reduction of beam width,[8,9] and multi-pixel detectors.[10]

In this paper we propose and theoretically study a compact GRIN lens suitable for fabrication of dense arrays of PCAs with individual integrated substrate lenses. In the proposed lens design, see Fig. 1(b)-1(c), a graded effective refractive index is obtained by sub-wavelength microstructuring of the PCA substrate, which advantageously also allows for an inexpensive monolithic fabrication process by deep reactive-ion etching (DRIE). Different microstructures in xy and yz planes are proposed due to polarization dependence of the effective refractive index for the same microstructure, as illustrated in Fig. 1(c). Other types of flat focusing THz optics has recently been proposed, including GRIN lenses based on metallic[11] and dielectric[12–14] metamaterials, and Fresnel zone plate lenses.[15,16] However, all of these had dimensions much larger than a typical PCA.

[a]Corresponding author: ts@nano.aau.dk

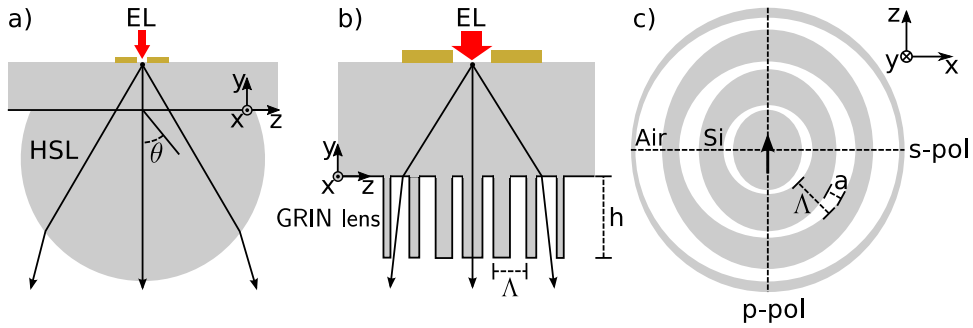

FIG. 1. Scheme of the proposed GRIN lens structure in comparison to a HSL. (a) PCA with a HSL mounted on the backside, (b) the proposed GRIN lens incorporated directly into the substrate. (c) A top down view of the GRIN structure where the arrow in the center represents the position and direction of the point-dipole. θ: angle used to calculate far-field radiation patterns, El: excitation laser beam, Λ: period of the GRIN structure, a: air-trench width, and h: height of the GRIN lens.

II. THEORETICAL APPROACH

Contrary to theoretical methods applied previously for ordinary THz lenses,[3,4] e.g. HSL's, the microstructuring proposed here requires that one applies a more rigorous solution of Maxwell's equations taking into account the full-wave nature of the radiation, reflections inside the lens, interference, etc. We address this here by using GFIEM.[17] Since this type of method is more involved than previously applied theoretical analysis in the realm of THz optics, we will give a brief explanation of one such method.

In the proposed design the radiation is generated by a dipole current source located at the bottom of a 400 μm thick layer of Si substrate with the GRIN lens placed on the other side. The point-dipole is a simple model of the burst of current generated when the small gap between the two biased electrodes of a PCA is illuminated with a short femtosecond pulse.[2] The dipole will be oriented along z, and as a result the dipole-emitted radiation will be purely s-polarized in the xy plane, and purely p-polarized in the yz plane, see Fig. 1(c). The analysis done is two-dimensional such that e.g. the z-axis is considered invariant for the s-polarized plane and vice versa. Silicon was chosen as the lens material due to its very low losses and dispersion in the THz range[18] and the possibility to use it as a growth substrate for GaAs[19] and low-temperature grown GaAs.[20]

A. Modelling method

The calculations presented throughout this paper were obtained using the Greens function area integral equation method (GFAIEM),[17] with the exception that the Greens function surface integral equation method (GFSIEM)[17] was applied for the HSL, as this method is better suited for structures with curved surfaces. Results obtained with the GFAIEM for other cases were also verified using the GFSIEM. A brief overview of the implementation of the GFAIEM used to analyze the GRIN lens in the s-polarized plane will be given here. For s-polarization, where the complex electric field in the xy plane will only have a z component, the total electric field $E^s(\mathbf{r})$ can be calculated by solving the following area integral equation

$$E^s(\mathbf{r}) = E_0^s(\mathbf{r}) + \int g(\mathbf{r},\mathbf{r}')k_0^2(\epsilon(\mathbf{r}') - \epsilon_{\text{ref}}(\mathbf{r}'))E^s(\mathbf{r}')\mathrm{d}A', \tag{1}$$

where $E_0^s(\mathbf{r})$ is the field generated by the dipole source in a reference structure consisting of the 400 μm thick substrate without the lens, k_0 is the free-space wave number, $\epsilon_{\text{ref}}(\mathbf{r})$ is the dielectric constant of the reference structure, and $\epsilon(\mathbf{r})$ is the dielectric constant of the total structure including the lens, and $g(\mathbf{r},\mathbf{r}')$ is the Greens function governing the field generated at $\mathbf{r}$ by a source at $\mathbf{r}'$ in the reference structure. In the p-polarized plane a vectorial expression similar to that in Eq. (1) is found for the vector field $\mathbf{E}^p(\mathbf{r})$. Eq. (1) was discretized into rectangular elements with assumed constant electric fields, and the expression was cast on matrix form and solved numerically using a

combination of a Fast Fourier Transform routine and an iterative solution scheme.[21,22] The Greens function used in Eq. (1) represents a single interface. It thus neglects the effect of light scattered by the lens geometry being reflected back from the interface located at $y = 400$ μm. The reference field $E_0^s(\mathbf{r})$ can for $y < 0$ be expressed as

$$E_0^s(\mathbf{r}) = -\omega^2\mu_0 p\frac{i}{2\pi}\int_0^{+\infty} k_{y,\mathrm{Si}}^{-1}\cos(k_x[x-x'])(t^s(k_x))^2 e^{-i(k_{y,\mathrm{air}}y'-k_{y,\mathrm{Si}}y)}\mathrm{d}k_x, \tag{2}$$

where p is the dipole moment, x' and y' define the dipole position, $t^s(k_x)$ is the Fresnel transmission coefficient for a single Si-air interface, and $k_{y,\alpha} = (k_0^2\epsilon_\alpha - k_x^2)^{1/2}$. The scalar Green's function used in Eq. (2) has an extra term $t^s = (1 + r^s)$ in the integrand, compared to a single interface Green's function, which takes into account one reflection occurring from the interface closest to where the dipole is located ($y = 400$ μm).[23] However, multiple reflections for radiation back and fourth in the Si-substrate were neglected, which is in line with previous work based on other methods.[3,4]

B. GRIN lens optimization

In order to determine the lens design we use as a starting point the refractive index distribution of a GRIN lens with a continuously varying refractive index profile

$$n_{\mathrm{eff}}(r) = n_{\mathrm{air}} + (n_{\mathrm{Si}} - n_{\mathrm{air}})\,\mathrm{sech}(gr), \tag{3}$$

where g is the gradient parameter and r is the distance from the center of the lens. The expression in Eq. (3), which was adapted from,[24] is typically used to calculate the index distribution for a radially symmetric focusing GRIN lens in the field of fiber-optics. We shall now seek to obtain a realistic microstructured GRIN lens with the same type of effective-index profile. We have chosen the GRIN lens to have a height of h= 100 μm, a diameter of 600 μm, and a period of $\Lambda = 25$ μm. The refractive index of air is set to unity, while the refractive index of Si is set to 3.418.[25] For each period we must now choose the width of the air-trench a. We set a restriction of $2.5\mu m \le a \le 19.5\mu m$ to stay within a realistic maximum aspect-ratio of 40 for air-trenches in Si or Si ridges in air, achieved by DRIE (see Ref. 26). For a given g we now use $n_{\mathrm{eff}}(r)$ for r in a given period to determine a. For both polarizations a is found from the effective dielectric constant of a periodic microstructure in the long-wavelength limit,[27] which for electric fields parallel and anti-parallel to an interface is given by

$$\epsilon_\parallel = \Lambda^{-1}((\Lambda - a)\epsilon_{\mathrm{Si}} + a\epsilon_{\mathrm{air}}) \quad \text{and} \quad \epsilon_\perp = \left[\Lambda^{-1}((\Lambda - a)\epsilon_{\mathrm{Si}}^{-1} + a\epsilon_{\mathrm{air}}^{-1})\right]^{-1}. \tag{4}$$

One can then use that $\epsilon_{\mathrm{eff}}^{\mathrm{s}} = \epsilon_\parallel$ for the s-polarized field, and for the p-polarized field we use a weighted average given by

$$\epsilon_{\mathrm{eff}}^{\mathrm{p}} = \frac{|E_{0,y}^{\mathrm{p}}|\epsilon_\parallel + |E_{0,z}^{\mathrm{p}}|\epsilon_\perp}{|E_{0,y}^{\mathrm{p}}| + |E_{0,z}^{\mathrm{p}}|}. \tag{5}$$

Since effective indices are calculated differently for s- and p-polarized fields, the optimum structure in xy and zy planes will differ. A given choice of g can now be converted into values of a for each period, and we can seek the value of g leading to the optimum far-field radiation pattern. The field outside the lens, including in the far-field, is obtained by first solving Eq. (1) for the field inside the lens, and then this field is used in Eq. (1) to generate the fields elsewhere.

III. RESULTS

Different lenses were optimized to out-couple maximum power within a half-angle, ϕ, from the y-axis. In Fig. 2 a plot of the absolute value of the electric near-field is shown for a GRIN lens with $\phi = 45°$. Complex interference patterns are visible inside the lens. In the p-polarized plane, the air-trenches are clearly visible since the perpendicular electric field component jumps across air-Si interfaces with a factor $\epsilon_{\mathrm{Si}}/\epsilon_{\mathrm{air}}$, while in the s-polarized plane the field is everywhere continuous

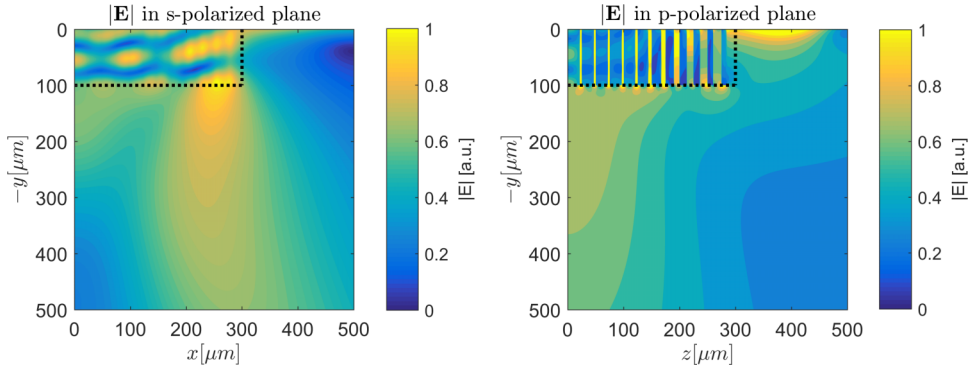

FIG. 2. Normalized magnitude of electric near-field in s- and p-polarized planes of the GRIN lens at a frequency of 1 THz and $\phi = 45°$. The gradient parameter in the s-polarized plane is $g^{s}_{45°} = 200^{-1}$, while $g^{p}_{45°} = 160^{-1}$ in the p-polarized plane. The dotted line indicates the boundary of the GRIN lens.

across interfaces. In Fig. 3(a)-3(b) the far-field radiation pattern from different GRIN lenses and a HSL can be seen. All the curves are relative to the Poynting vector at $\theta = 0°$ for the reference structure. The HSL had a distance of 2000 μm from the substrate to the tip of the lens, and its geometry was determined by the relations given in Ref. 4. Reflection losses due to the interface between the HSL and substrate were neglected. Comparing the radiation patterns for the GRIN lenses with different ϕ, for both s- and p-polarization, it can be seen that by altering the gradient parameter, the focusing properties can be changed significantly. However, by lowering the angle ϕ, the total power output is also lowered, which is illustrated by the insets. The insets show at which angles the main contribution of the radiation from the lenses is found compared to a substrate with no lens by $P_{90°}(\theta)$, where

$$P_{\beta}(\theta) = \frac{\int_0^{\theta} |S_{\mathrm{rel}}(r,\theta')| r \mathrm{d}\theta'}{\int_0^{\beta} |S_{\mathrm{rel},0}(r,\theta')| r \mathrm{d}\theta'}. \tag{6}$$

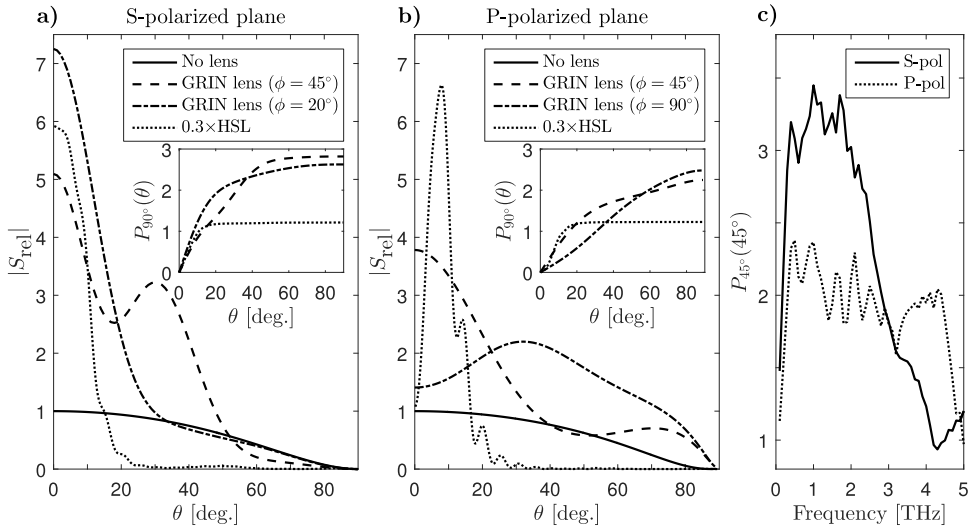

FIG. 3. Relative magnitude of Poynting vector at a distance of $400\lambda = 12$ cm from the substrate in a) the s- and b) p-polarized plane at a frequency of 1 THz. The insets shows $P_{90°}(\theta)$ as described in the text. The results for the HSL have been scaled by a factor of 0.3. The gradient parameters used are $g^{s}_{20°} = 140^{-1}$, and $g^{p}_{90°} = 260^{-1}$. No GRIN lens with $\phi = 90°$ is shown in a), since it yielded the same gradient parameter as when $\phi = 45°$, and the same is true for $\phi = 20°$ in b). c) illustrates the ratio between the power output from a PCA with an applied GRIN lens, with $\phi = 45°$, and the power output from a PCA without any lens at different frequencies in the THz range.

Here, S_{rel} and $S_{rel,0}$ are the Pointing vectors with and without a lens, respectively. It can be seen that the HSL produces a less diverging beam with a higher intensity on y-axis, in the s-polarized plane, with most of the radiation within an angle of approximately 15° from the y-axis. However, the overall power coupled out of the substrate, as seen in the inset, shows only a small advantage compared to the GRIN lenses. In the p-polarized plane, the HSL can be seen to exhibit unwanted interference effects with a large side lobe at approximately 8° with several following smaller lobes, which is a known disadvantage for this lens design.[4] In Fig. 3(c) the ratio $P_{45°}(45°)$ is plotted at different frequencies for a GRIN lens optimized for 1 THz with $\phi = 45°$. It shows the broadband nature of the proposed GRIN lens. This can be attributed to the all-dielectric design, which does not rely on any magnetic or electric resonances. This means that the effective bandwidth of the GRIN lens is only limited by the dispersion of the substrate and the dimensions of the microstructures. The GRIN lens enhances the out-coupled THz radiation from approximately 0.1 THz to 4 THz, which coincide well with the typical frequency range of commercially available THz spectrometers based on PCA technology.

IV. CONCLUSION

In conclusion, this work has demonstrated the very promising performance of a new type of microstructured GRIN substrate lenses for PCA's by applying Green's function integral equation methods. The proposed GRIN lenses show performances that are comparable with traditional HSL's, while opening up for the possibility of monolithic fabrication of densely packed PCA micro-arrays. It was also shown that the focusing properties of the GRIN lenses can be adapted by changing the gradient parameter, and that the effective bandwidth of the GRIN lenses spans from approximately 0.1 THz to 4 THz.

[1] M. V. Exter, C. Fattinger, and D. Grischkowsky, "Terahertz time-domain spectroscopy of water vapor," Opt. Lett. **14**, 1128 (1989).
[2] P. U. Jepsen, D. G. Cooke, and M. Koch, "Terahertz spectroscopy and imaging - Modern techniques and applications," Laser Photon. Rev. **5**, 124–166 (2011).
[3] P. U. Jepsen and S. R. Keiding, "Radiation patterns from lens-coupled terahertz antennas," Opt. Lett. **20**, 807–809 (1995).
[4] J. Van Rudd and D. M. Mittleman, "Influence of substrate-lens design in terahertz time-domain spectroscopy," J. Opt. Soc. Am. B **19**, 319 (2002).
[5] P. U. Jepsen, R. H. Jacobsen, and S. R. Keiding, "Generation and detection of terahertz pulses from biased semiconductor antennas," J. Opt. Soc. Am. B **13**, 2424 (1996).
[6] C. W. Berry, M. R. Hashemi, and M. Jarrahi, "Generation of high power pulsed terahertz radiation using a plasmonic photoconductive emitter array with logarithmic spiral antennas," Appl. Phys. Lett. **104**, 081122 (2014).
[7] N. Froberg and D. Auston, "Terahertz radiation from a photoconducting antenna array," IEEE J. Quantum Electron. **28**, 2291–2301 (1992).
[8] S. Preu, S. Malzer, G. H. Dohler, Q. Z. Zhao, M. Hanson, J. D. Zimmerman, A. C. Gossard, and L. J. Wang, "Interference between two coherently driven monochromatic terahertz sources," Appl. Phys. Lett. **92**, 221107 (2008).
[9] S. T. Bauerschmidt, G. H. Döhler, H. Lu, A. C. Gossard, S. Malzer, and S. Preu, "Arrayed free space continuous-wave terahertz photomixers," Opt. Lett. **38**, 3673–6 (2013).
[10] B. Pradarutti, R. Müller, W. Freese, G. Matthäus, S. Riehemann, G. Notni, S. Nolte, and A. Tünnermann, "Terahertz line detection by a microlens array coupled photoconductive antenna array," Opt. Express **16**, 18443–18450 (2008).
[11] J. Neu, B. Krolla, O. Paul, B. Reinhard, R. Beigang, and M. Rahm, "Metamaterial-based gradient index lens with strong focusing in the THz frequency range," Opt. Express **18**, 27748–27757 (2010).
[12] D. R. Smith, J. J. Mock, A. F. Starr, and D. Schurig, "Gradient index metamaterials," Phys. Rev. E **71**, 036609 (2005).
[13] N. Kundtz and D. R. Smith, "Extreme-angle broadband metamaterial lens," Nat. Mater. **9**, 129–132 (2010).
[14] S.-G. Park, K. Lee, D. Han, J. Ahn, and K.-H. Jeong, "Subwavelength silicon through-hole arrays as an all-dielectric broadband terahertz gradient index metamaterial," Appl. Phys. Lett. **105**, 091101 (2014).
[15] E. D. Walsby, J. Alton, C. Worrall, H. E. Beere, D. A. Ritchie, and D. R. S. Cumming, "Imprinted diffractive optics for terahertz radiation," Opt. Lett. **32**, 1141 (2007).
[16] S. Wang, T. Yuan, E. Walsby, R. J. Blaikie, S. M. Durbin, D. R. S. Cumming, J. Xu, and X.-C. Zhang, "Characterization of T-ray binary lenses," Opt. Lett. **27**, 1183 (2002).
[17] A. V. Lavrinenko, J. Lægsgaard, N. Gregersen, F. Schmidt, and T. Søndergaard, in *Numerical Methods in Photonics* (CRC Press, 2014), Chap. 7.
[18] J. Dai, J. Zhang, W. Zhang, and D. Grischkowsky, "Terahertz time-domain spectroscopy characterization of the far-infrared absorption and index of refraction of high-resistivity, float-zone silicon," J. Opt. Soc. Am. B **21**, 1379 (2004).
[19] J. E. Pedersen, S. R. Keiding, C. B. Sørensen, P. E. Lindelof, W. W. Ruhle, and X. Q. Zhou, "5-THz bandwidth from a GaAs-on-silicon photoconductive receiver," J. Appl. Phys. **74**, 7022–7024 (1993).
[20] R. Urata, D. Miller, and J. Harria, "Low-temperature growth of GaAs on Si used for ultrafast photoconductive switches," IEEE J. Quantum Electron. **40**, 800–804 (2004).

[21] B. T. Draine, "The discrete-dipole approximation and its application to interstellar graphite grains," Astrophys. J. **333**, 848 (1988).
[22] M. Petravic and G. Kuo-Petravic, "An ILUCG algorithm which minimizes in the euclidean norm," J. Comput. Phys. **32**, 263–269 (1979).
[23] W. Lukosz and R. E. Kunz, "Light emission by magnetic and electric dipoles close to a plane dielectric interface II Radiation patterns of perpendicular oriented dipoles," J. Opt. Soc. Am. **67**, 1615 (1977).
[24] K. Iga, "Theory for gradient-index imaging," Appl. Opt. **19**, 1039–1043 (1980).
[25] D. Grischkowsky, S. R. Keiding, M. van Exter, and C. Fattinger, "Far-infrared time-domain spectroscopy with terahertz beams of dielectrics and semiconductors," J. Opt. Soc. Am. B **7**, 2006 (1990).
[26] C. Brückner, T. Käsebier, B. Pradarutti, S. Riehemann, G. Notni, E.-B. Kley, and A. Tünnermann, "Broadband antireflective structures applied to high resistive float zone silicon in the THz spectral range," Opt. Express **17**, 3063 (2009).
[27] D. E. Aspnes, "Local-field effects and effective-medium theory: A microscopic perspective," Am. J. Phys. **50**, 704 (1982).